Structure and Energetics of Hydrogen Bonded HO_x−HNO_3 Complexes

Simone Aloisio and Joseph S. Francisco*

Department of Chemistry and Department of Earth and Atmospheric Sciences, Purdue University, West Lafayette, Indiana 47906

Received: March 29, 1999; In Final Form: May 21, 1999

In this work, we present our results of the study of the HO−HNO_3 complex. This complex is an important intermediate in the three-body reaction of hydroxyl radical and nitric acid. We have found that this intermediate is bound by 6.0 kcal mol $^{-1}$. The structure that we calculated is a six-membered ring. We also calculated vibrational and rotational frequencies for this complex. We have also studied a complex between HO_2 and HNO_3. This complex is stronger than the HO−HNO_3 intermediate with a binding energy of 9.5 kcal mol^{-1}.

I. Introduction

Nitric acid, HNO_3, is considered to be one of the main reservoirs of inorganic nitrate in the atmosphere. In the troposphere, it is formed by oxidation of NO and NO_2. Moreover, nitric acid is stable against photodissociation, with a photochemical lifetime estimated to be several weeks long.[1] As a result, nitric acid plays an important role in tropospheric chemistry.

Recent research has shown that nitric acid forms a complex with water in the gas phase.[2] Although the role of the nitric acid water complex has been extensively researched, the role of nitric acid complexes with radical species has not been as thoroughly examined. One such species that has received some attention is the nitric acid−hydroxyl radical complex. This complex has been suggested to be the involved in the reaction between HNO_3 and OH radical.

The reaction of nitric acid and hydroxyl radical

$$HNO_3 + OH \rightarrow H_2O + NO_3 \qquad (1)$$

has received much attention[3−13] both because of its importance as a loss process of HO_x in the lower stratosphere and because of its pressure and temperature dependencies. In the case of the reaction involving nitric acid and hydroxyl radical, the negative temperature dependence has been measured by many researchers.[1−11] The pressure dependence was first observed by Margitan and Watson[5] and later by Stachnick et al.[6] These data suggest that the reaction of HNO_3 and OH radical proceeds via a HO−HNO_3 complex. The structure of the complex is unknown. Moreover, there are no experimental or theoretical studies that indicate what the structure or the energetics of the complex is, although some theoretical work[14] has been done on the transition state. Experimental work by Singleton et al.[15] using deuterated nitric acid suggests that the complex may have a six-membered ring structure. In this work, we address the question of structure and energetics of the complex using ab initio molecular orbital calculations.

We have found that HO_2 forms a strongly bound complex with H_2O.[16] A question we raise is what is the possibility of a HO_2−HNO_3 complex. We explore the issue of whether it is likely that HO_2 and HNO_3 form a complex at least as strongly bound as the one between OH and HNO_3.

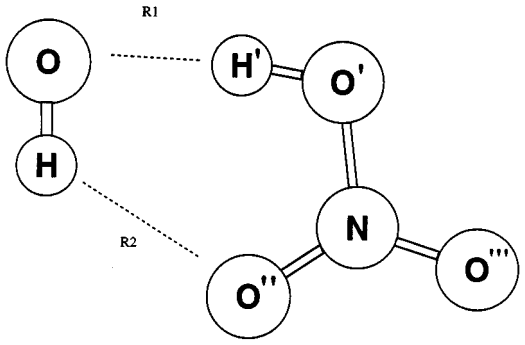

Figure 1. Optimized Structure for HO−HNO_3

II. Computational Methods

All calculations were performed using the GAUSSIAN 94[17] suite of programs. Geometries were optimized using the Becke three-parameter hybrid functional combined with Lee, Yang, and Parr correlation functional (B3LYP)[18] density functional theory method. This method has been shown to produce reliable geometry and vibrational frequency results for hydrogen bonded complexes when compared with other methods.[19,20] Basis sets employed are the 6-31G(d), 6-311++G(d,p), 6-311++G(2d,2p), and 6-311++G(3df,3pd). Frequency calculations were also performs at this level of theory. Zero-point energies taken from these frequency calculations can be assumed to be an upper limit due to the anharmonicity of the potential energy surface. Furthermore, single-point energies using the optimized geometries were calculated using coupled cluster theory including singlets, doublets, and triplets [CCSD(T)[21]]. As noted above, B3LYP calculations have been shown to predict geometries which are close to those predicted by coupled cluster methods, while the coupled cluster methods have been shown[22] to predict energies which are more reliable.

III. Results and Discussion

A. The HO−HNO_3 Complex. The structure of the HO−HNO_3 complex is shown in Figure 1. Our calculations support the structure first proposed by Margitan and Watson.[5] This is also the structure favored by the experiments of Singleton et al.[13] As can be seen in the figure, the six-membered ring is made up of the hydrogen, nitrogen, and two oxygens of the nitric acid and the hydroxyl radical. There is a hydrogen bond

10.1021/jp9910789 CCC: $18.00
Published on Web 07/14/1999

TABLE 1: B3LYP Optimized Geometry of the HO−HNO$_3$ Complex[a]

	basis set			
	6-31G(d)	6-311++ G(d,p)	6-311++ G(2d,2p)	6-311++ G(3df,3pd)
R1	1.799	1.838	1.822	1.814
R2	2.061	2.357	2.296	2.274
HO	0.991	0.980	0.980	0.980
H′O′	0.999	0.988	0.988	0.989
NO′	1.382	1.391	1.387	1.383
NO″	1.231	1.220	1.222	1.218
NO‴	1.202	1.196	1.196	1.193
H′OH	85.7	95.1	91.2	90.3
OHO″	130.6	116.3	120.7	121.8
HO″N	114.8	116.1	115.0	114.9
NO′H′	105.0	116.7	104.9	105.1
O′H′O	166.7	170.7	171.4	171.2
O′NO‴	114.9	114.7	114.8	114.8
O″NO‴	128.0	128.6	128.5	128.5
H′O′NO‴	180.0	180.0	180.0	180.0

[a] All bond distances are given in angstroms, all angles and dihedrals in degrees.

TABLE 2: B3LYP Optimized Geometries of Monomers[a]

	basis set			
	6-31G(d)	6-311++ G(d,p)	6-311++ G(2d,2p)	6-311++ G(3df,3pd)
		HNO_3		
H′O′	0.979	0.972	0.971	0.971
NO′	1.409	1.417	1.414	1.410
NO″	1.217	1.210	1.210	1.207
NO‴	1.203	1.194	1.195	1.191
NO′H′	102.7	103.4	103.0	103.2
O′NO‴	113.9	113.9	114.0	114.0
O″NO‴	130.4	130.4	130.4	130.4
H′O′NO‴	180.0	180.0	180.0	180.0
H′O′NO″	0.0	0.0	0.0	0.0
		Hydroxyl Radical		
OH	0.983	0.976	0.975	0.974
		Peroxyl Radical		
HO	0.984	0.977	0.975	0.975
OO	1.332	1.328	1.329	1.324
HOO	105.1	105.9	105.3	105.4

[a] All bond distances are given in angstroms, all angles and dihedrals in degrees.

between the hydrogen of the nitric acid and the oxygen of the hydroxyl radical and a similar but weaker one between the hydrogen of the hydroxyl radical and a terminal oxygen of the nitric acid. At the highest level of theory, these bond distances are 1.814 and 2.274 Å, respectively (Table 1). Comparisons can be made to the parent monomer geometries, which are given in Table 2. Both OH bonds are lengthened in the complex, as is the bond between the nitrogen and the terminal oxygen of the nitric acid, which is in the ring. The nitrogen's bond distance with the other terminal oxygen, which is outside of the ring, is relatively unaffected. The remaining oxygen is more closely bonded to the nitrogen in the complex than in the isolated nitric acid. Hence, this oxygen is bonding more strongly to the nitrogen and more weakly to the hydrogen than in the monomer. This is consistent with the formation of the products of this reaction, which are H_2O and NO_3.

The rotational constants for this complex are shown in Table 3. In this case, the rotational constants are 12390, 2831, and 2305 MHz for the rotational constants *A*, *B*, and *C*, respectively. This shows that the molecule is close to being an oblate symmetric rotor. This can be seen when looking at the structure of the intermediate in Figure 1.

TABLE 3: Rotational Constants for the HO−HNO$_3$ Complex[a]

	B3LYP			
	6-31G(d)	6-311++ G(d,p)	6-311++ G(2d,2p)	6-311++ G(3df,3pd)
A	12223	12271	12316	12390
B	2926	2796	2815	2831
C	2361	2277	2291	2305

[a] Rotational Constants are given in MHz.

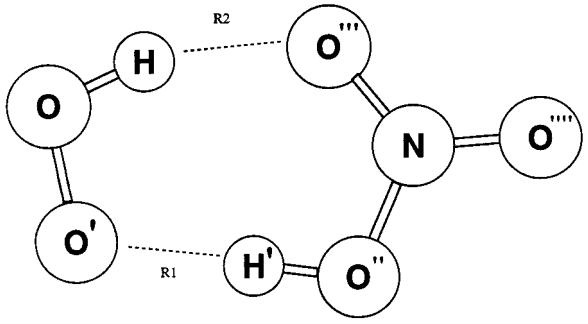

Figure 2. Optimized Structure for HO_2−HNO_3.

The vibrational frequencies and intensities of the complex are shown in Table 4. The structure has 10 intramolecular modes, which are in common with the parent monomers, and five new intermolecular modes. The shifts in the frequencies of these intramolecular modes are given in parentheses. These shifts are the difference in the complex's calculated frequencies and their parent monomers calculated frequencies at the same level of theory. Some of these modes are significantly shifted. For example, the OH stretch on the nitric acid has been shifted by 358 cm^{-1} to the red in the complex at the highest level of theory. This mode is also predicted to be the strongest absorber. Furthermore, at the highest level of theory, this mode is predicted to be 7.5 times more strongly absorbing than the same mode in the parent monomer. Some of the modes in the complex are predicted to be weaker absorbers than the similar modes in the parent monomers. For example, mode number 8 is expected to be a factor of 0.3 of its parent mode.

The binding energy of the HO−HNO_3 complex has been calculated at the CCSD(T)/6-311++G(2d,2p)//B3LYP/6-311++G(2d,2p) level of theory to be 6.0 kcal mol^{-1} lower than its parent including the zero-point energy. The calculated binding energies are shown in Table 5 for both the B3LYP and CCSD-(T) calculations. There were some significant differences in the binding energies when comparing these two methods using smaller basis sets. With the larger basis sets, there is better agreement between the two numbers. Using the 6-31G(d) basis set, for instance, the binding energy calculated is over 1.5 times that calculated using the larger basis sets. This is consistent with studies of other radical−molecule clusters using density functional theory in this lab. With the larger basis sets, there is better agreement between the two numbers.

B. The HO_2−HNO_3 Complex. We have calculated an optimized structure for the peroxyl radical−nitric acid complex. This is shown in Figure 2. The geometric parameters for this complex are given in Table 6. As can be seen, the structure is a seven-membered ring formed by the HO_2 and the H−O−N−O unit of the nitric acid. There are two hydrogen bonds that hold the ring together. The stronger one is that of the nitric acid as electron acceptor and the peroxyl radical as donor. This bond distance is 1.686 Å at the highest optimization. There is a similar, but slightly weaker, interaction between the hydrogen

TABLE 4: Vibrational Frequencies of the $HO-HNO_3$ Complex

		frequencies (shifts)[a]								intensity (relative to monomer)[b]							
mode	mode description	6-31G(d,p)		6-311++ G(d,p)		6-311++ G(2d,2p)		6-311++ G(3df,3pd)		6-31G(d,p)		6-311++ G(d,p)		6-311++ G(2d,2p)		6-311++ G(3df,3pd)	
1	OH stretch	3548	(−97)	3652	(−52)	3649	(−62)	3639	(−73)	125.5	(74)	57.3	(4.3)	70.5	(4.8)	72.2	(5.8)
2	O′H′ stretch	3297	(−369)	3396	(−329)	3382	(−352)	3365	(−358)	613.2	(8.0)	700.6	(6.8)	718.4	(7.2)	707.0	(7.5)
3	NO‴ stretch	1787	(−15)	1740	(−16)	1728	(−12)	1741	(−14)	302.4	(0.9)	402.1	(0.9)	363.1	(0.9)	336.7	(0.8)
4	NO′H′ bend	1480	(+133)	1435	(+86)	1443	(+97)	1447	(+96)	188.4	(0.6)	192.7	(0.6)	214.0	(0.7)	206.6	(0.7)
5	NO″ stretch	1352	(−21)	1325	(+5)	1321	(−3)	1327	(+4)	194.6	(4.6)	215.8	(4.1)	216.5	(3.0)	196.6	(4.2)
6	O″NO‴ bend	956	(+38)	928	(+31)	935	(+34)	939	(+35)	129.9	(0.8)	172.0	(0.9)	154.7	(0.8)	154.2	(0.8)
7	NO′O″O‴ umbrella	779	(+10)	189	(+10)	791	(+9)	797	(+10)	4.8	(0.4)	3.2	(0.4)	5.3	(0.6)	5.4	(0.6)
8	O′NO″ bend	680	(+27)	676	(+27)	676	(+27)	682	(+27)	2.8	(0.6)	6.7	(0.3)	4.1	(0.3)	4.0	(0.3)
9	NO′H′ wag	671	(+164)	581	(+118)	638	(+156)	668	(+173)	174.7	(1.3)	169.6	(1.2)	137.0	(1.1)	125.6	(1.1)
10	O′NO‴ bend	657	(+75)	627	(+41)	631	(+46)	637	(+48)	74.5	(7.8)	3.7	(0.6)	7.3	(1.0)	7.8	(1.1)
11	HOH′ asymmetric stretch	565		425		453		458		246.9		227.3		227.0		228.5	
12	O′HO bend	224		185		187		190		18.5		12.5		15.4		17.1	
13	HOH′ symmetric stretch	280		161		167		182		109.3		156.6		135.6		127.1	
14	OHO″ bend	181		111		113		113		27.3		41.3		40.6		41.6	
15	HOH′O′ torsion	81		70		73		76		1.1		3.8		3.1		2.7	

[a] Frequencies and shifts from monomers are in cm^{-1}. [b] Intensities and intensities relative to monomers are in km mol^{-1}.

TABLE 5: Relative Energies of the $HO-HNO_3$ Complex in kcal mol^{-1}

	B3LYP[a]		CCSD(T[b]	
basis set	D_e	D_o	D_e	D_o
6-31G(d)	11.4	9.6	9.7	7.9
6-311++G(d,p)	7.1	5.8	7.7	6.4
6-311++G(2d,2p)	6.9	5.6	7.3	6.0
6-311++G(3df,3pd)	6.9	5.6		

[a] From full optimization. [b] Single point using B3LYP optimized structure of same basis set.

TABLE 6: B3LYP Optimized Geometry of the HO_2-HNO_3 Complex[a]

	basis set			
	6-31G(d)	6-311++ G(d,p)	6-311++ G(2d,2p)	6-311++ G(3df,3pd)
R1	1.720	1.727	1.696	1.686
R2	1.779	1.810	1.775	1.757
NO‴	1.239	1.232	1.234	1.230
NO⁗	1.201	1.193	1.194	1.191
NO″	1.367	1.373	1.367	1.363
H′O″	1.007	1.000	1.002	1.003
HO	0.999	0.991	0.992	0.993
OO′	1.325	1.320	1.323	1.318
O‴HO	159.1	155.0	158.6	159.1
HOO′	104.1	104.7	104.2	104.2
OO′H′	109.1	112.1	109.4	109.0
H′O″N	105.9	105.9	106.1	106.3
O″NO‴	117.6	117.1	117.2	117.2
NO‴H	125.8	128.7	126.0	125.8
O‴NO⁗	126.8	127.2	126.9	126.9
O⁗NO‴H	0.0	0.0	0.0	0.0
O″NO‴H	180.0	180.0	180.0	180.0
O′OHO‴	0.0	0.0	0.0	0.0
H′O″NO‴	0.0	0.0	0.0	0.0
H′O″NO⁗	180.0	180.0	180.0	180.0
H′O′OH	0.0	0.0	0.0	0.0

[a] All bond distances are given in angstroms, all angles and dihedrals in degrees.

of the HO_2 and an oxygen of the HNO_3. This bond distance is 1.757 Å at the same level of theory. It is interesting that both of these bond distances are shorter than the primary hydrogen−oxygen bond in the $HO-HNO_3$ complex, implying stronger bonding in both cases. The intermolecular bond distances previously calculated by Tao et al.[2] for the H_2O-HNO_3 complex

TABLE 7: Rotational Constants for the HO_2-HNO_3 Complex[a]

	B3LYP			
	6-31G(d)	6-311++ G(d,p)	6-311++ G(2d,2p)	6-311++ G(3df,3pd)
A	9088	9143	9145	9200
B	1851	1851	1874	1888
C	1538	1539	1555	1567

[a] Rotational constants are given in MHz.

fall between those we have calculated for these complexes. All three complexes have a ring-type geometry.

When compared to the parent monomer geometries, there is a general pattern similar to the $HO-HNO_3$ complex in terms of which bonds are lengthened and shortened. Both hydrogen−oxygen bonds are lengthened in the complex. The bond between the terminal oxygen in the ring and the nitrogen in the nitric acid is slightly longer in the complex than the isolated HNO_3. The bond between the out-of-ring terminal oxygen and the nitrogen remains unaffected. The remaining oxygen−nitrogen bond in the nitric acid is shorter in the complex, as was the case for $HO-HNO_3$. The oxygen−oxygen bond of the peroxyl radical is slightly shorter in the complex than in isolated HO_2.

The calculated rotational constants for the HO_2-HNO_3 complex are shown in Table 7. As is the case in the $HO-HNO_3$ complex, this molecule is close to being an oblate symmetric rotor. Its rotational constants are 9200, 1888, and 1567 MHz at the highest optimized level of theory.

The vibrational frequencies for the peroxyl radical−nitric acid complex are shown in Table 8. Similar to the $HO-HNO_3$ complex, there is a large red shift in the OH stretch frequencies. In this case, the shift is predicted to be even larger than that in the former complex. The OH stretch in the nitric acid, for example, is predicted to be shifted to the red by 649 cm^{-1} at the highest level of theory. Comparably, the OH stretch in the peroxyl radical is predicted to be shifted by 280 cm^{-1} to the red. These shifts are 3.8 and 1.8 times larger than the analogous shifts in the hydroxyl radical-nitric acid complex. These modes have large calculated band strengths as well. For the nitric acid OH stretch, the intensity of this band is predicted to be 8.2 times larger than in the isolated monomer. This is very similar to the enhanced band strength in that same mode in the $HO-HNO_3$

TABLE 8: Vibrational Frequencies of the HO_2-HNO_3 Complex

		frequencies (shifts)[a]				intensity (relative to monomer)[b]			
mode	mode description	6-31G(d,p)	6-311++ G(d,p)	6-311++ G(2d,2p)	6-311++ G(3df,3pd)	6-31G(d,p)	6-311++ G(d,p)	6-311++ G(2d,2p)	6-311++ G(3df,3pd)
1	OH stretch	3326 (−200)	3386 (−210)	3354 (−262)	3322 (−280)	891.7 (100)	789.0 (30)	947.6 (33)	984.9 (24)
2	O′H′ stretch	3119 (−547)	3172 (−554)	3106 (−692)	3074 (−649)	605.5 (7.9)	756.4 (7.4)	798.3 (8.0)	771.9 (8.2)
3	NO″H′ bend	1789 (+442)	1748 (+262)	1742 (+395)	1751 (+428)	253.6 (5.9)	339.1 (1.1)	263.2 (0.86)	275.0 (5.9)
4	HOO′ bend	1562 (+107)	1515 (+92)	1548 (+107)	1551 (+115)	188.3 (5.0)	150.8 (5.0)	151.1 (4.0)	176.2 (4.5)
5	NO‴ stretch	1502 (−300)	1486 (−270)	1498 (−241)	1502 (−253)	159.0 (0.51)	198.1 (2.2)	261.1 (0.63)	223.4 (0.54)
6	NO‴ stretch	1340 (−33)	1303 (−17)	1300 (−24)	1305 (−46)	213.6 (5.0)	230.8 (4.4)	226.5 (3.1)	210.5 (0.69)
7	OO′ stretch	1232 (+54)	1209 (+52)	1218 (+51)	1224 (+55)	15.6 (0.58)	15.0 (0.52)	14.7 (0.51)	14.2 (0.50)
8	O″NO‴ bend	981 (+63)	958 (+61)	969 (+68)	974 (+70)	107.5 (23.9)	139.1 (0.69)	120.9 (0.65)	121.5 (0.66)
9	NO″H′ wag	809 (+302)	794 (+331)	858 (+377)	893 (+398)	46.1 (0.35)	13.8 (0.10)	52.6 (0.43)	49.1 (0.42)
10	NO″O‴O⁗ umbrella	771 (+2)	748 (+11)	787 (+5)	795 (+8)	37.3 (2.7)	74.5 (9.4)	17.3 (1.8)	12.6 (1.4)
11	O″NO‴ bend	694 (+41)	695 (+47)	696 (+47)	703 (+48)	3.8 (0.40)	5.7 (0.27)	5.7 (0.39)	5.8 (0.38)
12	O″NO⁗ bend	640 (+58)	639 (+53)	644 (+59)	650 (+61)	1.8 (0.40)	1.8 (0.27)	2.0 (0.27)	2.1 (0.30)
13	HO‴N wag	602	580	640	677	176.3	197.0	156.3	148.8
14	O′H′O″ bend	299	274	281	288	61.8	65.9	66.3	67.2
15	OHO‴ bend	213	198	206	209	5.4	9.0	10.8	9.9
16	H′O′O bend	197	175	176	183	0.8	0.9	0.7	0.6
17	HO‴NO⁗ torsion	95	93	96	98	4.0	3.9	3.2	2.9
18	H′O″NO⁗ torsion	67	69	73	76	0.0	0.1	0.0	0.1

[a] Frequencies and Shifts from Monomers are in cm^{-1}. [b] Intensities and Intensities relative to Monomers are in km $mole^{-1}$.

TABLE 9: Relative Energies of the HO_2-HNO_3 Complex in kcal mol^{-1}

	B3LYP[a]		CCSD(T[b]	
basis set	D_e	D_o	D_e	D_o
6-31G(d)	14.9	12.8	12.8	10.7
6-311++G(d,p)	11.3	9.3	11.7	9.8
6-311++G(2d,2p)	11.2	9.2		
6-311++G(3df,3pd)	11.7	9.5		

[a] From full optimization. [b] Single point using B3LYP optimized structure of same basis set.

complex. However, where the predicted intensity of the OH stretch in the hydroxyl radical complex is only 5.8 times larger than that the parent monomer, in the peroxyl radical complex, the OH stretch in the peroxyl radical is predicted to be 24 times larger than that the isolated HO_2. This is consistent with the larger perturbation in that mode due to the stronger bonding on that molecule. Because of this, the OH stretch on the nitric acid and that on the peroxyl radical are of comparable intensity in the HO_2-HNO_3 complex. The red shift and corresponding increase in intensity has also been predicted in the H_2O-HNO_3 complex.[2] The magnitude of these shifts, as well as the increased predicted band strengths of some of these same vibrational modes leads us to believe that the infrared region may be a good place to experimentally observe these complexes.

The calculated binding energy for the peroxyl radical−nitric acid complex is 9.5 kcal mol^{-1} at the highest level of theory, the B3LYP/6-311++G(3df,3pd) level (Table 9). This is considerably larger than that of the hydroxyl radical-nitric acid complex. This is due to the stronger bonding in the former complex, especially between the electron donor nitric acid oxygen/peroxyl radical hydrogen bond, but also at the electron donor peroxyl terminal oxygen/nitric acid hydrogen bond. As in the $HO-HNO_3$ complex, the latter bond is stronger than the former. However, in the HO_2-HNO_3 complex, the former bond is comparable in strength to the latter. As one might expect, the binding energy for H_2O-HNO_3 lies between that of the $HO-HNO_3$ and HO_2-HNO_3 complex.

C. Thermodynamic and Kinetic Stability of the Complexes. The thermodynamic data for the products of the reactions forming the complexes,

$$OH + HNO_3 \rightleftarrows HO-HNO_3 \quad (2)$$

$$HO_2 + HNO_3 \rightleftarrows HO_2-HNO_3 \quad (3)$$

can be calculated from the data obtained in the ab initio calculations. Room-temperature data for the reactants was taken from NASA's JPL Publication 97-4.[23] These data were extrapolated to other temperatures using Kirchhoff's law:

$$\Delta H(T_2) - \Delta H(T_1) = \Delta C_p \Delta T \quad (4)$$

where T is the temperature and ΔC_p is the difference in heat capacity at constant pressure of the substances whose enthalpy is being calculated to those of the elements in their natural state. Differences in heat capacities were assumed to be independent of temperature. Entropies were extrapolated to different temperatures using the following equation:

$$S(T_2) - S(T_1) = C_v \ln(T_2/T_1) \quad (5)$$

where C_v is the heat capacity at constant volume. The enthalpies of formation (ΔH_f) have been calculated for the complexes at 200 K and at 300 K. The $HO-HNO_3$ complex has a ΔH_f value of −29.9 kcal mol^{-1} at 300 K and a ΔH_f of −29.5 kcal mol^{-1} at 200 K. For HO_2-HNO_3, these values are −40.9 and −40.3 kcal mol^{-1} at 300 and 200 K, respectively. The entropy values for $HO-HNO_3$ at 300 and 200 K are 80.2 and 72.4 cal mol^{-1} K^{-1}, respectively. The entropies for HO_2-HNO_3 are 82.7 and 74.6 cal mol^{-1} K^{-1} at 300 and 200 K. We used these data to calculate equilibrium constants (K_f) for reactions 9 and 10 at 200 and 300 K. For $HO-HNO_3$, K_f^{300} is 4.3×10^{-21} cm^3 $molecule^{-1}$, and K_f^{200} is 6.6×10^{-19} cm^3 $molecule^{-1}$. One notes that the formation of the complex is favored by over 150 times at 200 K over formation at 300 K. For HO_2-HNO_3, K_f^{300} is 1.5×10^{-19} cm^3 $molecule^{-1}$ and K_f^{200} is 9.8×10^{-16} cm^3 $molecule^{-1}$. HO_2-HNO_3 formation is favored by over 6500 times at 200 K over formation at 300 K. In comparing formation constants for the complexes, one sees that the formation of HO_2-HNO_3 is much more favored than formation of HO−

HNO_3. This is especially true at lower temperatures. At 300 K, HO_2-HNO_3 has a K_f value that is over 30 times larger than that for $HO-HNO_3$, while at 200 K, K_f for HO_2-HNO_3 is about 1500 times greater than the same value for $HO-HNO_3$.

The dissociation constants (k_{diss}) for the complex can also be calculated using a method first developed by Troe[24,25] and further shown to be effective by Patrick and Golden[26] for reactions of atmospheric importance. The dissociation constant can be described by the following equation:

$$k_{diss} = Z_{LJ}\rho(E_0)RT(Q_{vib})^{-1}\exp(-E_0R^{-1}T^{-1})F_EF_{anh}F_{rot} \quad (6)$$

where Z_{LJ} is the Lennard-Jones collision frequency, $\rho(E_0)$ is the density of states, R is the gas constant, T is the temperature, Q_{vib} is the vibrational partition function for the associated species, E_0 is the critical energy, and F_E, F_{anh}, and F_{rot}, are correction terms for the energy dependence of the density of states, anharmonicity and rotation, respectively.

Using this method, the dissociation constant for $HO-HNO_3$, k_{-9}, is calculated to be 5.2×10^{-12} cm^3 molecule^{-1} s^{-1} at 300 K and 3.4×10^{-14} cm^3 molecule^{-1} s^{-1} at 200 K. The lifetime of the complex can be expressed as

$$\tau = (k_{diss}[M])^{-1} \quad (7)$$

where τ is the lifetime and [M] is the total number density of molecules. Taking the experiments of Margitan and Watson as an example, where a typical [M] would be about 3×10^{18} molecule cm^{-3}, τ would be about 60 ns at 300 K and about 10 μs at 200 K. For HO_2-HNO_3, k_{-10} has been calculated to be 1.1×10^{-13} and 2.0×10^{-17} cm^3 molecule^{-1} s^{-1} at 300 and 200 K, respectively. Using the same total number density as above, the lifetimes for HO_2-HNO_3 would be 3 μs at 300 K and 20 ms at 200 K.

Using the formation constants mentioned above, one can estimate the equilibrium concentrations of these complexes in the atmosphere. It can be quickly seen that these concentrations are quite low due to the low number densities of the monomer species. Under reasonable atmospheric conditions, one might expect number densities of 1×10^9 molecule cm^{-3} for HNO_3, 1×10^8 molecule cm^{-3} for HO_2, and 1×10^6 molecule cm^{-3} for OH. This corresponds to very low number densities of complex, regardless of temperature.

However, it is possible that this may happen under some laboratory conditions. In an experiment with number densities of 1×10^{12} molecule cm^{-3} for HO_2 and 1×10^{16} molecule cm^{-3} for HNO_3, the equilibrium concentration of HO_2-HNO_3 would be 1.5×10^9 molecule cm^{-3}. If the total number density was 1×10^{17} molecule cm^{-3}, the complex would have a lifetime of about 90 μs. If the same experimental conditions were possible at 200 K, the equilibrium concentration of the complex would be about 9×10^{11} molecule cm^{-3}. This corresponds to 90% of the HO_2 present. Furthermore, the lifetime for this complex would be about 500 ms. For this reason, the HO_2-HNO_3 complex may be observable in the gas phase.

IV. Conclusions

The structure and vibrational frequencies of the $HO-HNO_3$ complex have been presented. The six-membered ring structure proposed by Margitan and Watson[5] has been confirmed as the preferred conformation for $HO-HNO_3$. The energetics of this complex are consistent with what is observed in previous experiments. We have also studied the HO_2-HNO_3 complex in detail. This complex is predicted to be much more strongly bound than the $HO-HNO_3$ complex. We suggest that the HO_2-HNO_3 complex should be observable experimentally.

Acknowledgment. We thank the JPL Super-Computing Project for support of this research. The JPL Super-Computing Project is sponsored by the NASA Office of Space Science and Application. We also thank Dan Veitor, systems analyst of the Earth and Atmospheric Sciences department at Purdue University for his technical expertise.

References and Notes

(1) Liu, SC.; Trainer, M.; Fehsenfeld, F. C.; Parish, D. D.; Williams, E. J.; Fahey, J. W.; Hubler, G.; Murphy, P. C.; *J. Geophys. Res.;* **1987,** 92, 4191.

(2) Tao, F. M.; Higgens, K.; Klemperer, W.; Nelson, D. D.; *Geophy. Res. Lett.*, **1996**, 23, 1797.

(3) Kurylo, M. J.; Cornett, K. D.; Murphy, J. L.; *J. Geophys. Res.*, **1982**, 87, 3081.

(4) Wine, P. H.; Ravishankara, A. R.; Kreutter, N. M.; Shah, R. C.; Nicovich, J. M.; Thompson, R. L.; Wuebbles, D. J.; *J. Geo. Res.*, **1981**, 86, 1105−1112.

(5) Margitan, J. J.; Watson, R. T.; *J. Phys. Chem.*, **1982**, 86, 3819−3824.

(6) Marinelli, W. J.; Johnston, H. S.; *J. Chem. Phys.*, **1982**, 77, 1225−1234.

(7) Jourdain, J. J.; Poulet, G.; LeBras, G.; *J. Chem. Phys.*, **1982**, 76, 5827−5833.

(8) Ravishankara, A. R.; Eisele, F. L.; Wine, P. H.; *J. Chem. Phys.*, **1983**, 78, 1140−1144.

(9) Smith, C. A.; Molina, L. T.; Lamb, J. J.; Molina, M. J.; *Int. J. of Chem. Kinet.*, **1984**, 16, 41−45.

(10) Devolder, P.; Carlier, M.; Pauwels, J. F.; Sochet, L. R.; *Chem. Phys. Lett.*, **1984**, 111, 94−99.

(11) Jolly, G. S.; Paraskeropoulos, G.; Singleton, D. L.; *Chem. Phys. Lett.*, **1985**, 117, 132−137.

(12) Connell, P. S.; Howard, C. J.; *Int. J. of Chem. Kinet.*, **1985**, 17, 17.

(13) Stachnik, R. A.; Molina, M. J.; Molina, L. T.; *J. of Phys. Chem.*, **1986**, 90, 2777−2780.

(14) Lamb, J. J.; Mozurkewich, M.; Benson, S. W.; *J. Phys. Chem.*, **1989**, 88, 6441.

(15) Singleton, D. L.; Paraskevopoulos G.; Irwin, R. S.; *J. Phys. Chem.*, **1991**, 95, 694−697.

(16) Aloisio, S.; Francisco, J. S.; *J. Phys. Chem*, **1998**, 102, 1899−1902.

(17) GAUSSIAN 94, Revision D.2, Frisch, M. J.; Trucks, G. W.; Schlegel, H. B.; Gill, P. M. W.; Johnson, B. G.; Robb, M. A.; Cheeseman, J. R.; Keith, T.; Petersson, G. A.; Montgomery, J. A.; Raghavachari, K.; Al-Laham, M. A.; Zakrzewski, V. G.; Ortiz, J. V.; Foresman, J. B.; Cioslowski, J.; Stefanov, B. B.; Nanayakkara, A.; Challacombe, M.; Peng, C. Y.; Ayala, P. Y.; Chen, W.; Wong, M. W.; Andres, J. L.; Replogle, E. S.; Gomperts, R.; Martin, R. L.; Fox, D. J.; Binkley, J. S.; Defrees, D. J.; Baker, J.; Stewart, J. P.; Head-Gordon, M.; Gonzalez, C.; Pople, J. A.; **1995**, GAUSSIAN, Inc., Pittsburgh, PA.

(18) Becke, A. M.; *J. Chem. Phys.*, **1993**, 98, 5648.

(19) Kim, K.; Jordan, K. D.; *J. Phys. Chem.*, **1994**, 98, 10089−10094.

(20) Novoa, J. J.; Sosa, C.; *J. Phys. Chem.*, **1995**, 99, 1583715845.

(21) Raghavachari, K.; Trucks, G. W.; Pople, J. A.; Head-Gordon, M.; *Chem. Phys. Lett.*, **1989**, *157*, 479.

(22) Tsuzuki, S.; Uchimaru, T.; Tanabe, K.; *Chem. Phys. Lett.*, **1998**, 286, 202−208.

(23) DeMore, W. B.; Sander, S. P.; Golden, D. M.; Hampson, R. F.; Kurylo, M. J.; Howard, C. J.; Ravishankara, A. R.; Kolb, C. E.; Molina, M. J.; Chemical Kinetics and Photochemical Data for Use in Stratospheric Modelling, Evaluation No.12, **1997**, National Aeronautics and Space Administration-Jet Propulsion Laboratory, Pasadena.

(24) Troe, J.; *J. Chem. Phys.*,, **1977**, 66, 4745.

(25) Troe, J.;*J. Chem. Phys.*,, **1977**, 66, 4758.

(26) Patrick, R.,; Golden, D. M.; *Int. J. of Chem. Kinetics*, **1983**, 15, 1189−1227.